Vibrational Energy Relaxation of Water Molecules in a Hydrated Lithium Nitrate Crystal

Wilbert J. Smit and Huib J. Bakker*

FOM Institute AMOLF, Science Park 104, 1098 XG Amsterdam, The Netherlands

E-mail: bakker@amolf.nl

*To whom correspondence should be addressed

Abstract

Water molecules in hydrated salts often have a well-defined geometrical arrangement and form an excellent model system for studying the effects of the hydrogen-bond environment on vibrational energy relaxation. Hydrated lithium nitrate contains two distinct types of crystal water molecules. One water molecule makes strong and weak hydrogen bonds; the other water molecule makes two bifurcated hydrogen bonds. We use femtosecond two-dimensional infrared spectroscopy to probe the vibrational relaxation dynamics of the OD stretch vibration of dilute HDO molecules in lithium nitrate trihydrate. In the temperature range from 22 to 295 K we observe a decrease in vibrational lifetime from 3.8±0.2 to 2.8±0.1 ps for the strongly hydrogen-bonded species, from 5.41±0.08 to 4.14±0.05 ps for the bifurcated hydrogen-bonded species, and from 10.4±0.2 to 8.8±0.4 ps for weakly hydrogen-bonded species. This temperature dependence is opposite to that of the OD stretch vibration of dilute HDO:H_2O ice, for which the vibrational lifetime increases from 480±40 fs at 25 K to 850±60 fs at 265 K. We discuss the origin of this difference in temperature dependence.

Introduction

Water is an exceptional substance with many anomalous properties. Most of these anomalous properties are caused by the fact that the water molecules form an extended three-dimensional hydrogen-bond network. Infrared (IR) spectroscopy is a powerful tool to study the hydrogen-bonding interactions between water molecules as the frequency of the OH stretch vibrations strongly depends on the hydrogen-bond strength: the stronger the hydrogen bond, the lower its frequency.[1] In liquid water, a broad variation of hydrogen-bond strengths exists. The vibrational lifetime of the hydroxyl stretching modes shows a pronounced variation with frequency and thus with hydrogen-bond strength.[2–5] The underlying mechanism of the vibrational relaxation remains an active field of study.[4,6–10]

Recently, hydrated salts have emerged as a model system for studying the effects of the

hydrogen-bond environment on vibrational energy relaxation.[11–14] Crystal water in hydrated salts has a well-defined geometrical arrangement with an accordingly well-defined hydrogen-bond strength. The IR fingerprint of crystal water has recently led to the discovery of hydrated salts on Mars, demonstrating the presence of water on Mars.[15] Here we study the properties of water molecules present as crystal water in lithium nitrate trihydrate using femtosecond mid-infrared spectroscopy. Lithium nitrate contains crystal water with three different types of hydrogen bonds, leading to spectrally well-separated absorption lines of the OH stretch vibrations.[12,16,17] Lithium nitrate trihydrate is of interest as a thermal energy storage material because of its low melting point (30 °C) and its relatively large latent heat of fusion of 452 MJ/m^3 for the solid phase.[18–21]

The crystal structure of $LiNO_3{\cdot}3H_2O$ contains two different water species as illustrated in Fig. 1. The nitrate anion, lithium cation and one of the two non-equivalent water molecules lie in the crystal plane indicated as b in Fig. 1. This water molecule donates bifurcated hydrogen bonds to two oxygen atoms of a nitrate ion. Adjacent planes of type b are linked transversely by water molecules of the other type, forming the planes indicated as c in Fig. 1. One of the OH groups of this water molecule donates a relatively strong hydrogen bond to the water molecule in plane b, while the other OH group donates a relatively weak hydrogen bond to the nitrate ion. The vibrational lifetimes of the three distinct hydrogen-bonded OH stretch modes have been measured for HDO molecules in $LiNO_3{\cdot}HDO(D_2O)_2$ at a temperature of 220 K.[12,13]

In this work we study the temperature dependence of the vibrational energy relaxation of the three different hydroxyl vibrations. We perform this study by probing the OD stretch vibrations of HDO molecules embedded in $LiNO_3{\cdot}HDO(H_2O)_2$. We observe that the vibrational lifetime increases with decreasing temperature, opposite to what is observed for pure water and ice. We present a model that accounts for the observed temperature dependence of the relaxation.

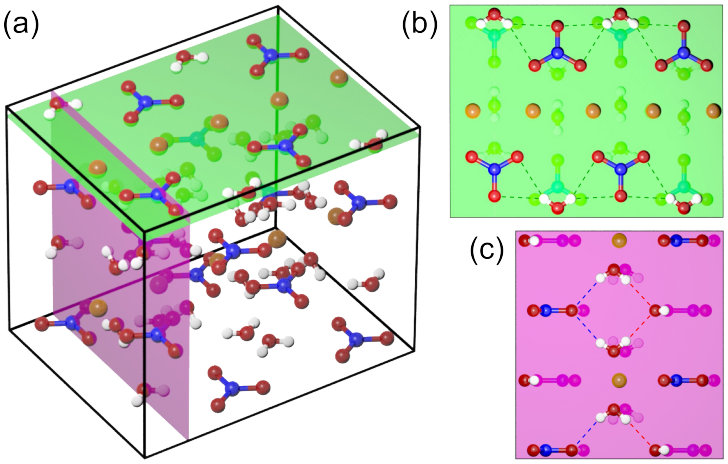

Figure 1: Crystal structure of lithium nitrate trihydrate.[22,23] The crystal structure belongs to the orthorhombic group D_{2h}^{17} (Cmcm) and has two different types of water molecules. The OH groups of the two types of water molecules lie in mutually perpendicular planes, which are projected in panels b and c for clarification. (b) Plane with the bifurcated hydrogen bonds (green dashed lines). (c) Plane with the strong hydrogen bonds (red dashed lines) and the weak hydrogen bonds (blue dashed lines). The colour scheme is as follows: H (white), Li (brown), N (blue), and O (red).

Experimental Methods

The lithium nitrate trihydrate samples are prepared as follows. A solution of 18.5 M $LiNO_3$ is dissolved in isotopically diluted water (10 % D_2O in H_2O). The $LiNO_3$ is fully dissolved by heating the solution above 304 K.[20] The solution is subsequently pressed between two z-cut sapphire windows without a spacer, resulting in a sample thickness of $\sim$5 μm. The hydrate is formed by lowering the temperature to 250 K in a closed cycle cryostat (CTI-Cryogenics) with a stability of 0.5 K. The lithium nitrate trihydrate crystal grows in a sprinkle shape from a nucleation point (see Fig. 2). Once the lithium nitrate trihydrate is formed, it remains stable up to its melting temperature of 303.3 K.[20]

By recording polarized IR transmission spectra of the sample using a FTIR microscope (Bruker Vertex 80v with Hyperion 3000) we have found that the macroscopic structure of the sample (Fig. 2) directly reflects the crystal orientation. The polarized linear spectra are shown in Fig. 3 and will be discussed in more detail below. The water molecules do-

nating bifurcated hydrogen bonds lie in the plane perpendicular to the needle lines. The water molecules forming strong and weak hydrogen bonds lie in the plane parallel to the needle lines and perpendicular to the bifurcated water molecules hydrogen bonds. We measure unpolarized linear absorption spectra of the sample at different temperatures with a PerkinElmer 881 double-beam IR spectrometer.

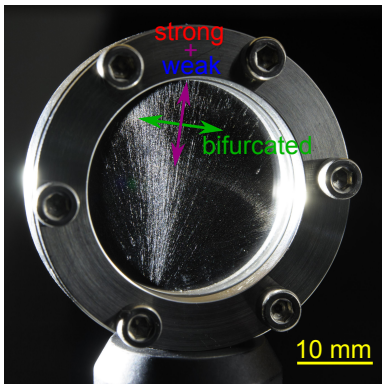

Figure 2: Lithium nitrate trihydrate crystal grown in a sprinkle shape from a nucleation point and the visible structure of the sample indicates the crystal orientation (see text).

We study the vibrational dynamics of the OD stretch vibrations of the HDO molecules in the lithium nitrate crystal with two-dimensional infrared (2D-IR) spectroscopy. These measurements are performed in the temperature range 22–295 K. The transient absorption of the OD stretch vibrations is measured as a function of the excitation and detection frequencies and as a function of the time delay between the excitation and detection pulses. The excitation from the ground state $v = 0$ to the first excited $v = 1$ state results in a transient spectrum. For each vibration this transient spectrum consists of a bleaching component, due to ground state depletion and stimulated emission of the $1 \rightarrow 0$ transition, and an induced absorption component corresponding to the $1 \rightarrow 2$ transition. The $1 \rightarrow 2$ transition has a lower frequency than the fundamental $0 \rightarrow 1$ transition because the vibrational potential of the OD stretch vibration is anharmonic.

We use a commercial femtosecond Ti:sapphire laser system (Coherent Evolution) delivering 3.7 mJ pulses at a wavelength of 800 nm and at a repetition rate of 1 kHz to generate

mid-infrared pulses at ∼4 μm that are resonant with the OD stretch vibrations of HDO. Approximately two-thirds of the laser output is used to generate the excitation pulse, and one-third is used to generate the detection pulse. The excitation pulse is generated with a commercial optical parametric amplifier (Spectra-Physics OPA-800C) with an additional amplification stage in β-barium borate (BBO). The generated signal and idler pulses are subsequently difference frequency mixed in $AgGaS_2$ yielding pulses in the mid-IR spectral region. The excitation pulse has a central wavelength of 3.9 μm (2570 cm^{-1}), a spectral bandwidth with a full width at half maximum (FWHM) of 410 nm (270 cm^{-1}), and a pulse energy of ∼20 μJ. The pump pulse is sent into a Mach–Zehnder interferometer. The mirror in one of the two arms of the interferometer is placed on a motorized stage and its position is controlled with a fast scanning routine, as described by Helbing and Hamm.[24] The delay between the two split excitation pulses is tracked with a HeNe beam aligned above the IR beams and a quadrature counter. One interferometric output is focused to a spot size of ∼150 μm in the sample. The other interferometer output is focused onto a pyroelectric detector (Eltec 420M7-27) to record a linear interferogram of the pump pulse, which is used to calculate the absolute delay between the two pump pulses.

The detection pulse is generated in a home-built optical parametric amplifier with two BBO-based amplification stages. The generated signal and idler pulses are used in a difference frequency mixing process in a $AgGaS_2$ crystal to produce 3 μJ pulses at 4.0 μm (2500 cm^{-1}) with a FWHM of 600 nm (370 cm^{-1}). Using wedged ZnSe plates we split off two ∼200 nJ pulses of the generated pulse. These pulses are the detection pulse and the reference pulse. The detection pulse is guided over a motorized delay stage to vary its time delay with respect to the excitation pulse. The detection and the reference pulses are focussed to a spot of ∼100 μm at different positions in the sample. The detection pulse is spatially overlapped with the excitation pulse in the sample. The detection pulse has the same direction of polarization as the excitation pulse.

Delay time zero is determined in a Ge plate and the cross-correlation time between the

excitation and the detection pulses is ∼250 fs. The reference is used to correct for pulse-to-pulse intensity and spectral fluctuations. After passing the sample the detection and the reference beams are dispersed with an Oriel monochromator and their spectrally resolved intensities are measured by two 32 pixel liquid-N_2-cooled mercury cadmium telluride (MCT) arrays. The pump frequency axis in the 2D spectrum is generated by Fourier transformation of the signal as a function of the delay between the two excitation pulses. Before Fourier transformation the time-domain is zero padded by a factor of 2 and multiplied with a Hamming window function.[25,26] The 2D-IR setup is purged with nitrogen gas to reduce the strong CO_2 absorption around 2345 cm^{-1}. A librating CaF_2 window around the Brewster angle phase-cycles the excitation pulse to average out interference effects between the detection pulse and scattered light of the excitation pulse.[27]

Results

In Fig. 3 we present linear infrared absorption spectra for two distinct polarization directions of the infrared light. The spectra show the three distinct kinds of HDO molecules in the hydrated lithium nitrate crystal. We find a frequency of 2501 cm^{-1} with a FWHM of 23 cm^{-1} for the stretch vibration of the OD group with a strong hydrogen bond, 2563 cm^{-1} with a FWHM of 29 cm^{-1} for the stretch vibration of the OD group with a bifurcated hydrogen bond, and 2610 cm^{-1} with a FWHM of 9 cm^{-1} for the stretch vibration of the OD group with a weak hydrogen bond. The peak at 2463 cm^{-1} can be assigned to a combination of two stretch vibrations of the nitrate ion.[28] The cross section of the nitrate band is low in comparison with the OD modes; therefore, it is not observed in the nonlinear spectrum because the transient absorption response scales approximately with the cross section squared. The observation that the OD modes can be completely suppressed by changing the polarization points out that the crystal grows in such a way that planes b and c in Fig. 1 are perpendicular to the window.

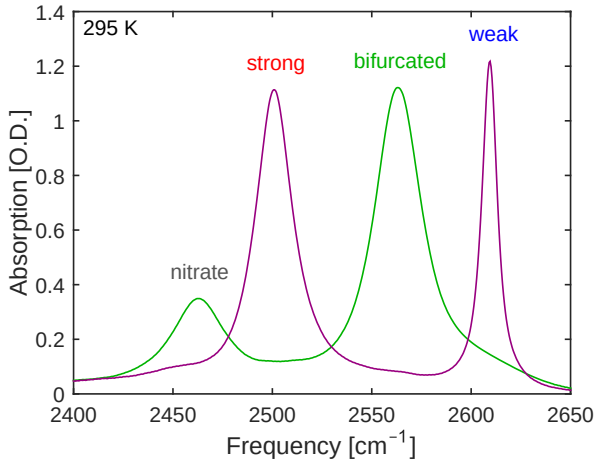

Figure 3: Polarized linear spectra at 295 K. In one polarization direction the OD stretch modes with strong and weak hydrogen bonds are observed (purple). In the other polarization direction the bifurcated hydrogen-bonded OD stretch modes are observed (green).

We measure 2D-IR spectra with the excitation and detection pulses polarized parallel to the plane of the OD groups with strong and weak hydrogen bonds and with the excitation and detection pulses polarized parallel to the plane of the OD groups with bifurcated hydrogen bonds. The spectra are measured at eight different temperatures. In Fig. 4 we present 2D-IR spectra measured at temperatures of 22 and 295 K for a delay of 0.5 ps between the excitation and the detection pulses.

In Fig. 5 we show transient absorption spectra for excitation frequencies that correspond to the maxima of the bleaching signals of the weakly, bifurcated, and strongly bonded OD groups shown in the 2D spectra of Fig. 4. Besides the $0 \rightarrow 1$ bleaching signals, the transient spectra also show the presence of the $1 \rightarrow 2$ excited state absorption bands. These bands are red-shifted with respect to the fundamental $0 \rightarrow 1$ transition by 139 cm^{-1} for the OD group with a strong hydrogen bond, 110 cm^{-1} for the OD group with a bifurcated hydrogen bond, and 107 cm^{-1} for the OD group with a weak hydrogen bond. The $1 \rightarrow 2$ excited state absorption bands are about 2–3 times broader than the $0 \rightarrow 1$ bleaching signals. Possible explanations for this additional broadening are the short vibrational lifetime of the $v = 2$ state[25] and the quantum nature of the hydrogen bonds[29].

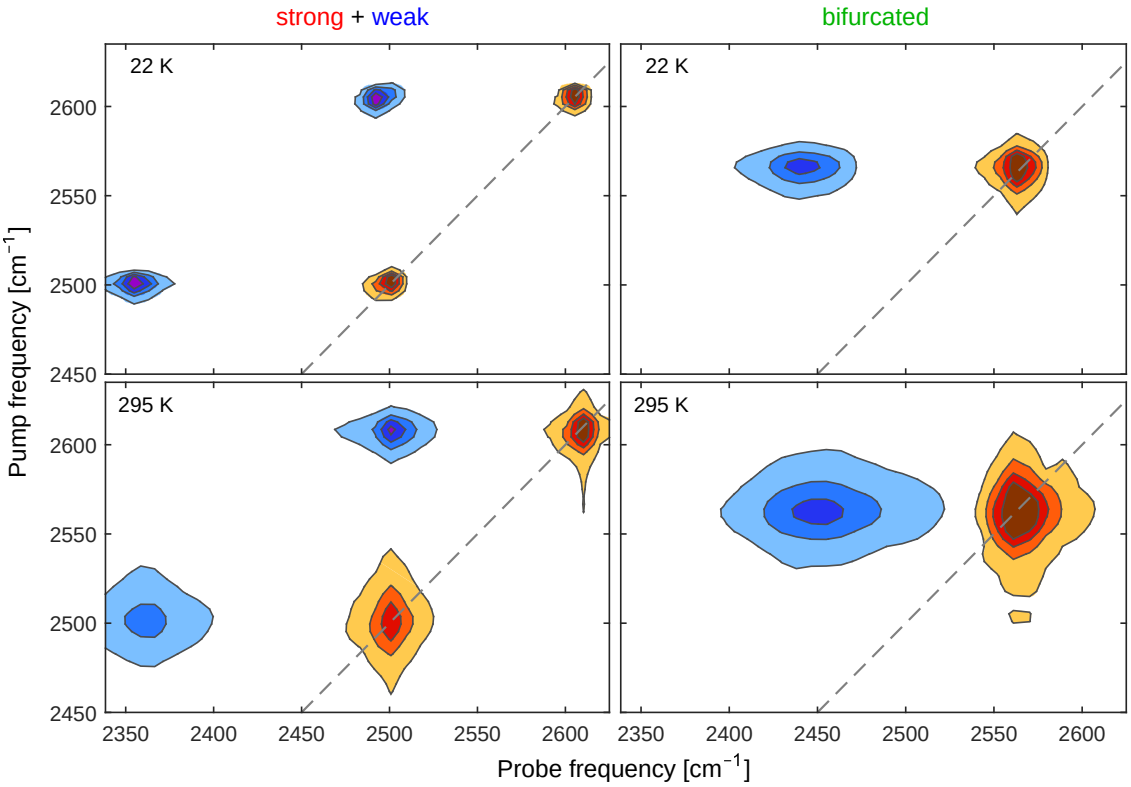

Figure 4: 2D-IR spectra at 22 and 295 K of the strongly and weakly hydrogen-bonded OD groups (left) and the bifurcated hydrogen-bonded OD groups (right). The delay between the excitation and the detection pulses is 0.5 ps. The positive absorption changes are shown in red, and the negative absorption changes are shown in blue. The colour steps correspond to a 10 % intensity increase and are truncated at 70 % of the maximal transient absorption differences. The spectra show distinct resonances and no cross-peaks.

The vibrational lifetimes are determined by fitting the decay of the $1 \rightarrow 2$ excited state absorption signals.[30] For this purpose the areas of the $1 \rightarrow 2$ induced absorption bands are integrated for each delay time. The resulting signal is plotted as a function of delay and fitted between 0.5 and 100 ps with a population relaxation model in which the vibration decays exponentially and a heating effect grows in with the same rate.[9] In Fig. 6 we present delay traces at 22 and 295 K. The vibrational lifetimes T_1 resulting from the fit are listed in Table 1. The errors represent 95 % confidence intervals of the fitting procedure.

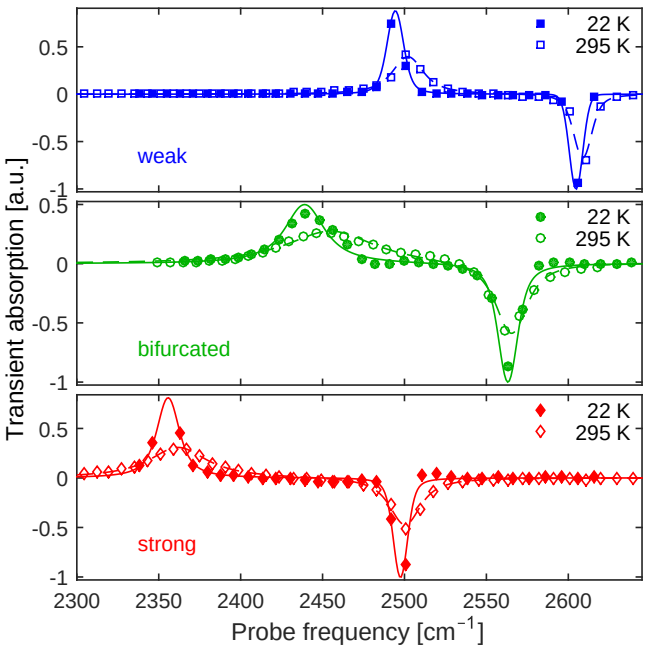

Figure 5: Normalized slices at excitation frequencies that correspond to the maximal bleaching signals of the weakly, bifurcated, and strongly bonded OD groups of the 2D spectra from Fig. 4. The transient spectra are fitted by two Lorentzian functions at 22 K (solid line and filled points) and at 295 K (dashed line and open points).

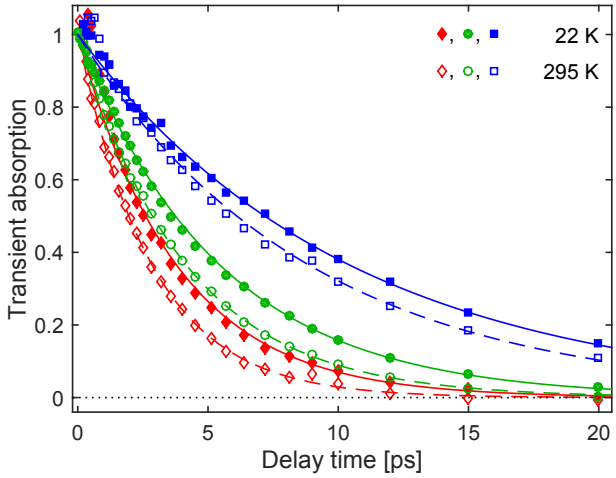

Figure 6: Fitted normalized absorption changes as a function of delay for the OD groups with strong (red), bifurcated (green) and weak (blue) hydrogen bonds, at 22 K (solid line and filled points) and at 295 K (dashed line and open points).

Discussion

From Table 1 it is clear that the vibrational lifetime of the OD stretch vibration in lithium nitrate trihydrate is shorter for the OD groups with strong hydrogen bonds than that for

Table 1: T_1 vibrational lifetimes of the three different hydrogen-bonded OD stretch vibrations of HDO in lithium nitrate trihydrate at different temperatures.

Temperature [K]	T_1 [ps]		
	strong	bifurcated	weak
22	3.8 ± 0.2	5.41 ± 0.08	10.4 ± 0.2
60	3.6 ± 0.1	5.2 ± 0.2	9.9 ± 0.3
100	3.47 ± 0.05	5.2 ± 0.2	10.8 ± 0.2
140	3.30 ± 0.08	5.1 ± 0.1	7.8 ± 0.8
180	3.3 ± 0.1	4.6 ± 0.1	10.3 ± 0.9
220	3.1 ± 0.2	4.5 ± 0.1	9 ± 2
250	3.13 ± 0.08	4.35 ± 0.07	9.1 ± 0.3
295	2.8 ± 0.1	4.14 ± 0.05	8.8 ± 0.4

the OD groups with bifurcated hydrogen bonds, which are in turn shorter than that for the OD groups with weak hydrogen bonds. This observation agrees with the typical behaviour of the hydroxyl stretch vibration of decreasing vibrational lifetime with increasing hydrogen-bond strength, as observed in bulk liquid water,[2–5] frozen reverse micelles,[31] and zeolites.[32] We find that the vibrational lifetimes of the OD stretch vibrations of HDO molecules in lithium nitrate trihydrate are ∼3 times larger than the lifetimes of the OH stretch vibration, which are at 220 K 1.1 ± 0.1, 1.9 ± 0.2, and 3.4 ± 0.3 ps for strongly, bifurcated, and weakly hydrogen-bonded OD groups, respectively.[13]

We observe a decrease of the vibrational lifetime with increasing temperature for all three hydrogen-bonded OD stretching modes. The vibrational energy relaxation rate is determined by the coupling and spectral overlap with (combination tones) of other modes that accept the energy. For the OD vibration of HDO molecules in dilute HDO:H_2O ice, the temperature dependence of the vibrational lifetime of the OD stretching vibration in ice could be well accounted for by considering the temperature dependence of the spectral overlap of the excited OD vibration and a single accepting combination mode.[9]

Using Fermi's golden rule, the relaxation rate of the OD stretch vibration (v_1) to a single

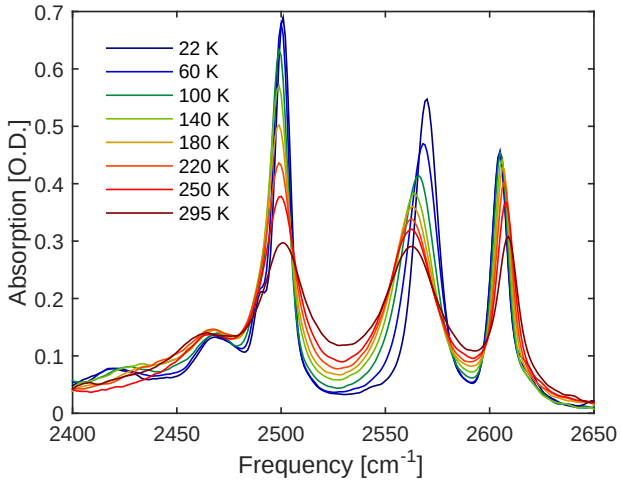

Figure 7: Unpolarized linear infrared absorption spectra of $LiNO_3{\cdot}HDO(H_2O)_2$ at different temperatures. The line widths of the OD stretch vibrational absorption bands increase with increasing temperature.

accepting (combination) mode can be expressed as

$$\begin{aligned}\frac{1}{T_1} &= \frac{2\pi}{\hbar}\iint d\omega\, d\omega'\, |\langle f|\hat{V}_{v_1,a}|i\rangle|^2 g_{v_1}(\omega)\rho_a(\omega')\delta(\omega-\omega') \\ &= \frac{2\pi}{\hbar}\int d\omega\, |\langle f|\hat{V}_{v_1,a}|i\rangle|^2 g_{v_1}(\omega)\rho_a(\omega),\end{aligned} \tag{1}$$

where $g_{v_1}(\omega)$ is the spectral distribution of the OD stretch vibration ($\int d\omega\, g_{v_1}(\omega) = 1$), $\rho_a(\omega)$ the density of states of the acceptor mode, and $\langle f|\hat{V}_{v_1,a}|i\rangle$ the coupling matrix element between the final and initial states. The Dirac delta function ensures conservation of energy. In this expression we assume rapid spectral diffusion due to fluctuations in the thermal bath. Assuming the density of states of the acceptor mode to be proportional to its spectral distribution, i.e. $\rho_a(\omega) \propto g_a(\omega)$, and the coupling strength to be independent of frequency, we arrive at

$$\frac{1}{T_1} \propto |\langle f|\hat{V}_{v_1,a}|i\rangle|^2 \int d\omega\, g_{v_1}(\omega) g_a(\omega). \tag{2}$$

When the two spectral distributions have Lorentzian line shapes, the overlap integral can be

Table 2: Peak positions (ω_{v_1}) and FWHM line widths (Γ_{v_1}) of the three different hydrogen-bonded OD stretch vibrations of HDO in lithium nitrate trihydrate at different temperatures determined from the linear spectra shown in Fig. 7.

T [K]	strong		bifurcated		weak	
	ω_{v_1} [cm^{-1}]	Γ_{v_1} [cm^{-1}]	ω_{v_1} [cm^{-1}]	Γ_{v_1} [cm^{-1}]	ω_{v_1} [cm^{-1}]	Γ_{v_1} [cm^{-1}]
22	2501	8	2570	13	2605	8
60	2500	9	2568	17	2605	8
100	2499	10	2566	20	2605	8
140	2499	12	2564	22	2606	8
180	2499	15	2563	24	2606	8
220	2499	18	2562	26	2607	9
250	2500	21	2563	28	2608	10
295	2500	30	2562	34	2609	12

solved analytically, i.e.

$$\int d\omega \, g_{v_1}(\omega) g_a(\omega) = \frac{2}{\pi} \frac{\Gamma_{v_1} + \Gamma_a}{4(\omega_{v_1} - \omega_a)^2 + (\Gamma_{v_1} + \Gamma_a)^2}, \tag{3}$$

where ω_{v_1} and Γ_{v_1} are the centre frequency and FWHM of the OD stretch mode, and ω_a and Γ_a denote the centre frequency and FWHM of the acceptor mode. The relaxation rate of the OD stretch vibration is then proportional to

$$\frac{1}{T_1} \propto |\langle f|\hat{V}_{v_1,a}|i\rangle|^2 \int d\omega \, \frac{\Gamma_{v_1} + \Gamma_a}{4(\omega_{v_1} - \omega_a)^2 + (\Gamma_{v_1} + \Gamma_a)^2}. \tag{4}$$

We fit the experimentally observed vibrational relaxation rates with a model in which we assume that the three OD groups relax to the same acceptor mode. This acceptor mode is assumed to have a Lorentzian shape and to be temperature independent. We fit the spectral position and the width of the acceptor mode. In the fitting, we calculate the spectral overlap of the three OD vibrations with the acceptor mode. The positions and widths of the OD stretch modes are determined from the linear spectra shown in Fig. 7 and given in Table 2. In the fitting, we take the value of the coupling strength $|\langle f|\hat{V}_{v_1,a}|i\rangle|^2$ to be equal for the strong and the weak hydrogen bonds, as they are situated on the same type of water molecules

in the crystal structure. The coupling matrix element of the bifurcated hydrogen-bonded OD group is allowed to be different from that of the strong and weak hydrogen bonds.thre The results of the fit are plotted in Fig. 8. We find the ratio of the coupling strengths of the strong/weak:bifurcated hydrogen bonds to be 1:1.3. The accepting mode resulting from the fit is centred at 2354 ± 12 cm^{-1} with a FWHM of 65 ± 17 cm^{-1}. Thus, the three OD modes and the found accepting mode only weakly overlap. Therefore, the OD modes and the accepting modes are only brought into resonance due to spectral diffusion caused by thermal bath fluctuations. We do not observe any IR active mode in the spectral range 2200–2400 cm^{-1}. However it is likely that the accepting mode is a combination band composed of several excitation quanta in different vibrations, which makes it invisible in the infrared and Raman spectra. The HDO and H_2O bending modes have frequencies of about 1460 cm^{-1} and 1650 cm^{-1}, respectively.[33] Therefore it appears likely that the accepting mode is a combination of the $v = 1$ of the HDO or H_2O bending mode in combination with one or two quanta in low-frequency intermolecular modes.

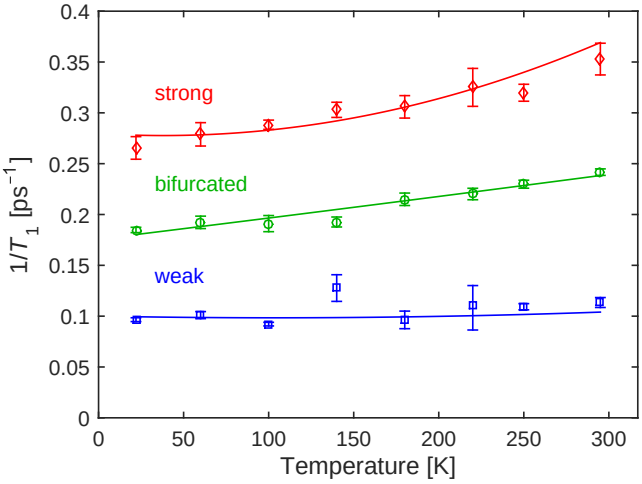

Figure 8: Vibrational lifetimes of the OD stretch vibrations of HDO molecules in three different hydrogen-bond configurations in lithium nitrate trihydrate as a function of temperature. The lifetimes are fitted utilizing Eq. (4), using the central frequencies and line widths of the different OD vibrations obtained from the linear absorption spectra, which yields a Lorentzian-shaped accepting mode centred at 2354 ± 12 cm^{-1} with a FWHM of 65 ± 17 cm^{-1}.

The observed temperature dependence is opposite to what has been observed for the

vibrational lifetime of the OD stretch vibration of HDO molecules in dilute HDO:H_2O ice,[9] for which the vibrational lifetime increases from 480±40 fs at 25 K to 850±60 fs at 265 K. For HDO:H_2O ice, the line width of the OD stretch increases with increasing temperature, and the peak position of the excited OD stretch vibration increases from 2415 cm^{-1} at 20 K to 2447 cm^{-1} at 270 K, i.e. 0.13 cm^{-1}/K on average.[9] As a result, the spectral overlap of the absorption band of the OD vibration with the absorption band of the bending and libration combination mode decreases, thus explaining the increase of the vibrational lifetime with increasing temperature. For $LiNO_3$·$HDO(H_2O)_2$ the change in peak position of the OD vibrations with temperature is one order of magnitude smaller than for dilute HDO:H_2O ice; hence, the change of the vibrational lifetime is dominated by the increase of the line width rather than the peak position (see Table 2). As this line width increases with temperature, the overlap with a combination band of the bending and low-frequency modes increases, which thus explains the observed decrease of the vibrational lifetime with increasing temperature.

In studies of the vibrational relaxation of hydroxyl groups in crystals[34,35] the relaxation was described to occur via crystal vibrations that are assumed to be harmonic. The temperature dependence of the relaxation was described with the multi-phonon relaxation model of Nitzan et al.[36,37] In this model the accepting mode is formed by a combination tone that consists of a number of low-frequency phonon excitations. The model describes a strong increase in the vibrational relaxation rate with temperature as a result of the increased thermal occupation of the harmonic phonon modes. Due to the harmonic character of the phonon modes, the vibrational amplitudes of these modes increase when they are thermally excited, and these larger amplitudes lead to an increase of the anharmonic coupling with the excited hydroxyl vibration, thus accelerating the vibrational relaxation.

Following the model of Nitzan et al.[36,37] the value of the coupling matrix element $\langle f|\hat{V}_{v_1,a}|i\rangle$ of Eq. (4) is expected to increase with temperature, because the accepting modes get thermally excited. We did not include such a temperature dependence in modelling the data,

and assumed the coupling matrix element to be temperature independent. For all three OD vibrations the temperature dependence of T_1 can be well explained from the temperature dependence of the spectral overlap of the excited OD vibrations and an accepting mode that likely consists of a bending mode in combination with low-frequency intermolecular modes of the water molecule (librations, hydrogen-bond stretch vibrations). For this accepting mode the coupling matrix element is indeed expected to show very little temperature dependence in the temperature range 22–295 K. The HDO and H_2O bending modes have frequencies of about 1460 cm^{-1} and 1650 cm^{-1}, respectively,[33] both being much larger than the thermal excitation energy k_BT (corresponding to 205 cm^{-1} at 295 K). This implies that the thermal excitation of the bending mode is negligible over the whole studied temperature range of 22–295 K. Hence, an increase in temperature from 22 to 295 K will lead to a negligible thermal excitation of this mode and thus negligible acceleration of the vibrational relaxation. The intermolecular librational and hydrogen-bond modes have much lower frequencies and their thermal occupation will increase in the studied temperature range. However, these modes are strongly anharmonic, showing a double-well potential,[38,39] which means that the vibrational amplitude will not strongly increase when the temperature is raised. Hence, for an accepting mode that consists of the $v = 1$ state of the bending mode and a few quanta of excitation in low-frequency intermolecular water modes, the assumption of a temperature independent coupling appears to be justified, at least at relatively low temperatures up to 295 K.

The present results show that the vibrational relaxation mechanism of the OH stretching vibrations of water is quite anomalous, even when the water molecules are contained in a highly-ordered crystal structure. While most high-frequency vibrations, like covalently bound hydroxyl vibrations,[34,35] relax via multi-phonon decay, following the relaxation model of Nitzan et al.[36,37], water molecules relax via the bending mode vibration in combination with anharmonic low-frequency intermolecular modes. This relaxation mechanism leads to a very different temperature dependence of the relaxation that in some cases, e.g. neat

water,[9,30,40] even leads to a deceleration of the relaxation with temperature.

Conclusions

We studied the vibrational dynamics of the OD stretch vibrations of HDO molecules in lithium nitrate trihydrate. Water molecules are located in the hydrated lithium nitrate crystal at specific positions, leading to hydroxyl groups with three different well-defined hydrogen-bond interaction strengths, including hydroxyl groups with strong hydrogen bonds, weak hydrogen bonds, and bifurcated (intermediate) hydrogen bonds. We measured the vibrational lifetimes of the OD stretch vibrations over a wide temperature range from 22 to 295 K. The vibrational lifetime of the strongly hydrogen-bonded OD groups is shorter than that for the bifurcated hydrogen-bonded OD groups, which in turn is shorter than that for the weakly hydrogen-bonded OD groups. For all three types of OD groups, the vibrational lifetime decreases with increasing temperature: from 3.8±0.2 ps at 22 K to 2.8±0.1 ps at 295 K for the strongly hydrogen-bonded species, from 5.41±0.08 ps at 22 K to 4.14±0.05 ps at 295 K for the bifurcated hydrogen-bonded species, and from 10.4±0.2 ps at 22 K to 8.8±0.4 ps at 295 K for the weakly hydrogen-bonded species. This temperature dependence can be well explained from an increase in the line width of the OD stretch absorption bands with increasing temperatures and the resulting increase in spectral overlap with a single (combination) accepting mode centred at 2354 ± 12 cm^{-1} with a FWHM of 65 ± 17 cm^{-1}. This accepting mode likely consists of the $v = 1$ state of the H_2O or HDO bending vibration in combination with one or two quanta in low-frequency intermolecular modes.

Acknowledgement

This work is part of the research program of the "Stichting voor Fundamenteel Onderzoek der Materie (FOM)", which is financially supported by the "Nederlandse organisatie voor Wetenschappelijk Onderzoek (NWO)". The authors thank Hinco Schoenmaker for technical

support, Yves Rezus for helpful discussions, Oleg Selig for the infrastructure of the data analysis, and Ricardo Struik for helping to make Fig. 1.

References

(1) Maréchal, Y. *The Hydrogen Bond and the Water Molecule*; Elsevier, 2007.

(2) Woutersen, S.; Emmerichs, U.; Bakker, H. J. Femtosecond Mid-IR Pump-Probe Spectroscopy of Liquid Water: Evidence for a Two-Component Structure. *Science* **1997**, *278*, 658–660.

(3) Gale, G.; Gallot, G.; Lascoux, N. Frequency-dependent vibrational population relaxation time of the OH stretching mode in liquid water. *Chem. Phys. Lett.* **1999**, *311*, 123–125.

(4) Lawrence, C. P.; Skinner, J. L. Vibrational spectroscopy of HOD in liquid D_2O. VII. Temperature and frequency dependence of the OH stretch lifetime. *J. Chem. Phys.* **2003**, *119*, 3840–3848.

(5) van der Post, S. T.; Hsieh, C.-S.; Okuno, M.; Nagata, Y.; Bakker, H. J.; Bonn, M.; Hunger, J. Strong frequency dependence of vibrational relaxation in bulk and surface water reveals sub-picosecond structural heterogeneity. *Nat. Commun.* **2015**, *6*, 8384.

(6) Deàk, J. C.; Rhea, S. T.; Iwaki, L. K.; Dlott, D. D. Vibrational energy relaxation and spectral diffusion in water and deuterated water. *J. Phys. Chem. A* **2000**, *104*, 4866–4875.

(7) Lawrence, C. P.; Skinner, J. L. Vibrational spectroscopy of HOD in liquid D_2O. I. Vibrational energy relaxation. *J. Chem. Phys.* **2002**, *117*, 5827–5838.

(8) Kandratsenka, A.; Schroeder, J.; Schwarzer, D.; Vikhrenko, V. S. Nonequilibrium molecular dynamics simulations of vibrational energy relaxation of HOD in D_2O. *J. Chem. Phys.* **2009**, *130*, 174507.

(9) Smit, W. J.; Bakker, H. J. Anomalous temperature dependence of the vibrational lifetime of the OD stretch vibration in ice and liquid water. *J. Chem. Phys.* **2013**, *139*, 204504.

(10) Liu, H.; Wang, Y.; Bowman, J. M. Ab Initio Deconstruction of the Vibrational Relaxation Pathways of Dilute HOD in Ice Ih. *J. Am. Chem. Soc.* **2014**, *136*, 5888–5891.

(11) Pandelov, S.; Pilles, B. M.; Werhahn, J. C.; Iglev, H. Time-Resolved Dynamics of the OH Stretching Vibration in Aqueous NaCl Hydrate. *J. Phys. Chem. A* **2009**, *113*, 10184–10188.

(12) Werhahn, J. C.; Pandelov, S.; Xantheas, S. S.; Iglev, H. Dynamics of Weak, Bifurcated, and Strong Hydrogen Bonds in Lithium Nitrate Trihydrate. *J. Phys. Chem. Lett.* **2011**, *2*, 1633–1638.

(13) Bradler, M.; Werhahn, J. C.; Hutzler, D.; Fuhrmann, S.; Heider, R.; Riedle, E.; Iglev, H.; Kienberger, R. A novel setup for femtosecond pump–repump–probe IR spectroscopy with few cycle CEP stable pulses. *Opt. Express* **2013**, *21*, 20145–20158.

(14) Hutzler, D.; Werhahn, J. C.; Heider, R.; Bradler, M.; Kienberger, R.; Riedle, E.; Iglev, H. Highly Selective Relaxation of the OH Stretching Overtones in Isolated HDO Molecules Observed by Infrared Pump–Repump–Probe Spectroscopy. *J. Phys. Chem. A* **2015**, *119*, 6831–6836.

(15) Ojha, L.; Wilhelm, M. B.; Murchie, S. L.; McEwen, A. S.; Wray, J. J.; Hanley, J.; Masse, M.; Chojnacki, M. Spectral evidence for hydrated salts in recurring slope lineae on Mars. *Nat. Geosci.* **2015**, *8*, 829–832.

(16) Pandelov, S.; Werhahn, J. C.; Pilles, B. M.; Xantheas, S. S.; Iglev, H. An Empirical Correlation between the Enthalpy of Solution of Aqueous Salts and Their Ability to Form Hydrates. *J. Phys. Chem. A* **2010**, *114*, 10454–10457.

(17) Muniz-Miranda, F.; Pagliai, M.; Cardini, G.; Righini, R. Bifurcated Hydrogen Bond in Lithium Nitrate Trihydrate Probed by ab Initio Molecular Dynamics. *J. Phys. Chem. A* **2012**, *116*, 2147–2153.

(18) van Essen, V. M.; Cot Gores, J.; Bleijendaal, L. P. J.; Zondag, H. A.; Schuitema, R.; Bakker, M.; van Helden, W. G. J. *Proceedings of the ASME 3rd International Conference of Energy Sustainability*; American Society of Mechanical Engineers, 2009; Vol. 2; pp 825–830.

(19) Balasubramanian, G.; Ghommem, M.; Hajj, M. R.; Wong, W. P.; Tomlin, J. A.; Puri, I. K. Modeling of thermochemical energy storage by salt hydrates. *Int. J. Heat Mass Transfer* **2010**, *53*, 5700–5706.

(20) Shamberger, P. J.; Reid, T. Thermophysical Properties of Lithium Nitrate Trihydrate from (253 to 353) K. *J. Chem. Eng. Data* **2012**, *57*, 1404–1411.

(21) Cabeza, L. F.; Gutierrez, A.; Barreneche, C.; Ushak, S.; Fernández, A. G.; Fernádez, A. I.; Grágeda, M. Lithium in thermal energy storage: A state-of-the-art review. *Renew. and Sust. Energ. Rev.* **2015**, *42*, 1106–1112.

(22) Hermansson, K.; Thomas, J. O.; Olovsson, I. Hydrogen bond studies. CXX. An X-ray determination of the crystal structure of $LiNO_3.3H_2O$. *Acta Crystallogr. Sect. B* **1977**, *33*, 2857–2861.

(23) Hermansson, K.; Thomas, J. O.; Olovsson, I. Hydrogen bond studies. CXXXVIII. Neutron diffraction studies of $LiNO_3.3H_2O$ at 120 and 295 K. *Acta Crystallogr. Sect. B* **1980**, *36*, 1032–1040.

(24) Helbing, J.; Hamm, P. Compact implementation of Fourier transform two-dimensional IR spectroscopy without phase ambiguity. *J. Opt. Soc. Am. B* **2011**, *28*, 171–178.

(25) Hamm, P.; Zanni, M. *Concepts and Methods of 2D Infrared Spectroscopy*; Cambridge University Press, 2011.

(26) Bartholdi, E.; Ernst, R. R. Fourier spectroscopy and the causality principle. *J. Magn. Resonance* **1973**, *11*, 9–19.

(27) Bloem, R.; Garrett-Roe, S.; Strzalka, H.; Hamm, P.; Donaldson, P. Enhancing signal detection and completely eliminating scattering usingquasi-phase-cycling in 2D IR experiments. *Opt. Express* **2010**, *18*, 27067–27078.

(28) Tsuboi, M.; Hisatsune, I. C. Infrared Spectrum of Matrix-Isolated Nitrate Ion. *J. Chem. Phys.* **1972**, *57*, 2087–2093.

(29) Perakis, F.; Widmer, S.; Hamm, P. Two-dimensional infrared spectroscopy of isotope-diluted ice Ih. *J. Chem. Phys.* **2011**, *134*, 204505.

(30) Lock, A. J.; Bakker, H. J. Temperature dependence of vibrational relaxation in liquid H_2O. *J. Chem. Phys.* **2002**, *117*, 1708–1713.

(31) Dokter, A. M.; Petersen, C.; Woutersen, S.; Bakker, H. J. Vibrational dynamics of ice in reverse micelles. *J. Chem. Phys.* **2008**, *128*, 044509.

(32) Brugmans, M. J. P.; Bakker, H. J.; Lagendijk, A. Direct vibrational energy transfer in zeolites. *J. Chem. Phys.* **1996**, *104*, 64–84.

(33) Falk, M. Frequencies of H–O–H, H–O–D and D–O–D bending fundamentals in liquid water. *J. Raman Spectrosc.* **1990**, *21*, 563–567.

(34) Casassa, M. P.; Heilweil, E. J.; Stephenson, J. C.; Cavanagh, R. R. Time-resolved measurements of OH(v=1) vibrational relaxation on SiO_2 surfaces: Isotope and temperature dependence. *J. Chem. Phys.* **1986**, *84*, 2361–2364.

(35) Fujino, T.; Kashitani, M.; Fukuyama, K.; Kubota, J.; Kondo, J.; Wada, A.; Domen, K.; Hirose, C.; Wakabayashi, F.; Kano, S. Population lifetimes of the OH stretching band of water molecules on zeolite surfaces. *Chem. Phys. Lett.* **1996**, *261*, 534–538.

(36) Nitzan, A.; Jortner, J. Electronic relaxation of small molecules in a dense medium. *Mol. Phys.* **1973**, *25*, 713–734.

(37) Nitzan, A.; Mukamel, S.; Jortner, J. Some features of vibrational relaxation of a diatomic molecule in a dense medium. *J. Chem. Phys.* **1974**, *60*, 3929–3934.

(38) Lippincott, E. R.; Schroeder, R. One-Dimensional Model of the Hydrogen Bond. *J. Chem. Phys.* **1955**, *23*, 1099–1106.

(39) Tayal, V. P.; Srivastava, B. K.; Khandelwal, D. P.; Bist, H. D. Librational Modes of Crystal Water in Hydrated Solids. *Appl. Spectrosc. Rev.* **1980**, *16*, 43–134.

(40) Woutersen, S.; Emmerichs, U.; Nienhuys, H. K.; Bakker, H. J. Anomalous Temperature Dependence of Vibrational Lifetimes in Water and Ice. *Phys. Rev. Lett.* **1998**, *81*, 1106–1109.